INTERPRETATION OF DAMAGE TO HOUSES AND CASUALTIES RELIED ON A PRECISE EVALUATION OF EARTHQUAKE GROUND MOTIONS IN THE EPICENTRAL REGION

— THE 1945 MIKAWA EARTHQUAKE —

Hitoshi TANIGUCHI

Research Associate, Faculty of Engineering, Aichi Institute of Technology

Fusanori MIURA

Associate Professor, Faculty of Engineering, Yamaguchi University

Toshio MOCHIZUKI

Professor, Center For Urban Studies, Tokyo Metropolitan University

and

Osamu INADA

Assistant Manager, Chubu Electric Power CO., INC.

(Received 2 May, 1988 and in revised form 1 August, 1988)

ABSTRACT

Although about two thousand people were killed by the 1945 Mikawa earthquake, a clear description of the entire event has yet to be given because the earthquake took place just before the end of World War II. In order to describe what happened in the epicentral region during this earthquake, the authors estimated the ground motion and investigated the damage done to houses the casualties caused by the earthquake.

The ground motion was estimated by a nonlinear finite element method, in which modified joint elements were adopted to model the fault plane. The seismic intensity in the area near the fault was estimated from the calculated maximum velocity. The damage done to houses and the casualties caused were investigated by questionnaire. The destruction of houses was compared in detail to the number of casualties. The type of damage is discussed in relation to the estimated ground motion.

1. INTRODUCTION

The Mikawa area in eastern Aichi Prefecture was struck by a strong earthquake at 3:38 A.M. January 13, 1945. About two thousand people were killed, more than fifteen hundred dwelling wooden houses completely collapsed, and more than eleven thousand non-dwellings partially destroyed [1]. Moreover, a considerable number of people were injured during the partial and total destruction of wooden houses by the earthquake. Although this was a major disaster, no clear description of the entire event was made because it took place at the end of World War II and its scale was hidden from the public. There has been an investigative report made that describes the damaged houses, ground destruction, casualties, etc. [2]; but, it contains ambiguous statements concerning where there were liquefied sites and the causes of casualties.

KEY WORDS: Mikawa earthquake, Nonlinear dynamic analysis, Rupture mechanism, Liquefaction, Damage of wooden houses

To determine what actually happened in the epicentral region during the earthquake, the authors first estimated the ground motion near the fault, investigated the characteristics of the disaster, then evaluated the relation between ground motion and the number and types of damaged houses and casualties. Ground motion was estimated by analyzing the fault model, the damage and casualties by questionnaire.

In the past two decades, the investigation of fault rupture mechanisms has been progressed remarkably. One commonly used theoretical approach by which the generation of seismic waves from a fault is analyzed is the "dislocation" theory. Most methods of this type are based on the elastic wave transmission theory in a half space. Various fault parameters such as rupture velocity, magnitude of final dislocation and source-time function, that are needed in this method are assumed in advance of numerical calculation, as are the geometrical parameters needed to describe the fault rupture process.

In an actual fault plane rupture begins, however, at some point on the plane then is transmitted. This produces successive ruptures in adjacent regions because the area of the rupture zone is governed by the stress field and the strength of the fault plane. Furthermore, the fault parameters mentioned above are not the source but the result of rupture.

Because of this, Toki and Miura [3] proposed a new technique with which to simulate the fault rupture process. It is based on the nonlinear finite element method in which a modified joint element is used to model the fault plane. In their method only two parameters are necessary; the distributions of the yield stress and the stress drop on the fault plane.

The authors investigated the rupture mechanism and the strong ground motion produced by the 1945 Mikawa earthquake in the Mikawa area using Toki and Miura's method. To simulate the rupture mechanism, we used the fault model proposed by Ando [4]. The crust-fault structure was determined from data gathered from explosion tests made in the Mikawa region [5,6].

As more than forty years have passed since the Mikawa earthquake, it is impossible to directly investigate the disaster that it caused. Therefore, a questionnaire was sent out to gather information on the extent of the disaster. Sixteen hundred and sixteen replies were collected, from which the distributions of liquefied places and the ratio of destroyed houses to the loss of life were obtained. These distributions are discussed in the relation to the estimated ground motion.

2. METHOD OF ANALYSIS

A flow chart showing how the authors estimated the near field ground motion and investigated the extent of the disaster caused by that motion is given in Fig. 1. The procedure had three main steps: (1) modeling of the crust-fault system with the finite element model; (2) calculation by static analysis of the initial stress field caused by the tectonic force and simulation of the fault rupture process by the nonlinear dynamic finite element method; and (3) discussion of the relation between ground motion and the extent of the disaster caused by the Mikawa earthquake. In the second step, the resultant dislocation at ground surface was compared with the recorded value, iteration of the calculation being continued until the difference between the calculated and observed dislocations became very small. As the method of analysis used is the same as that proposed in an earlier study [3], the process is given briefly.

2.1. *Modeling the fault*

The fault was modeled by arrangement of the modified joint element shown in Fig. 2. The relation between shearing stress and deformation is shown in Fig. 3. It is linear for a stress lower than τ_y, the yield stress. When τ reaches τ_y, the element yields and the shear stress decreases instantaneously to the residual strength, τ_r, because of the dynamic stress drop, $\Delta\tau_d$. Hereafter, the stress drop, $\Delta\tau$, is defined by $\Delta\tau=\tau_0-\tau_r$, in which, $\Delta\tau_0$ is the initial stress. The crust was modeled with two dimensional isoparametric elements.

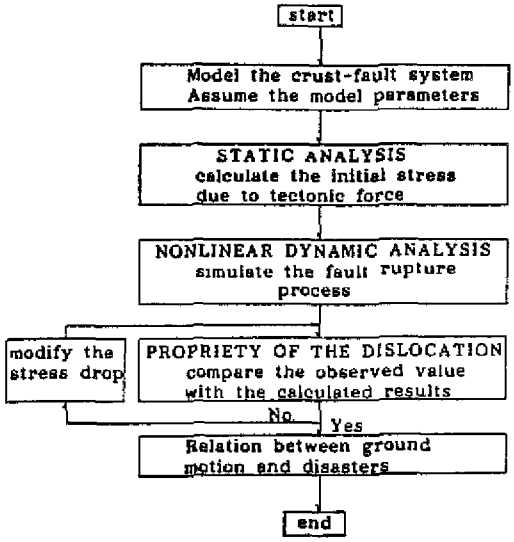

Fig. 1 Flow chart of the study.

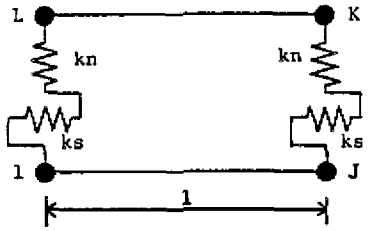

Fig. 2 Schematic representation of a modified joint element.

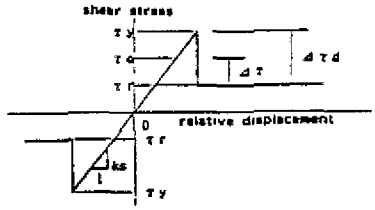

Fig. 3 Constitutive relation of the joint element.

2.2. *Procedure for analysis of fault rupture*

A static analysis was made to obtain the initial shear stress produced by the tectonic force along the fault. Lateral force was applied to both sides of the model as the tectonic force. This lateral force was increased until the induced shear stress reached the yield shear stress at some point on the fault; that was the origin of rupture. A dynamic analysis then was made in which the stress field determined in the previous step was used as the initial stress condition. The external force, in the first iteration in integrating the governing equation of motion, was the nodal forces equivalent to the dynamic stress drop of the joint element that corresponds to the original rupture. Strain energy was released by the first rupture as an elastic wave, and stress in the neighboring field was increased causing successive ruptures in those elements. In this way, rupture continued serially satisfying the governing equation of the crust-fault system. The only parameters that needed to be assigned to the fault were the shear strength and the stress drop. Therefore, the method does not assume other fault parameters such as fault rupture velocity, source-time function, final dislocation, etc. These values were obtained from the results of the simulation.

Integrating the equation of motion, the authors adopted Newmark's β method and assigned a value of 1/4 to β. The load transfer method was the scheme of numerical integration.

3. MODELING THE FAULT OF THE 1945 MIKAWA EARTHQUAKE

The fault of the 1945 Mikawa earthquake and the structure of the crust near this fault are shown in Fig. 4. The structure below ground was determined from explosion tests [5, 6]. The geometrical figure of the fault determined by Ando [4] was adopted. The width was 11 km, the length 12 km, and the dip angle about 30 degrees. The final dislocation of the fault was recorded as about 2.2 m at ground surface. Therefore, the authors repeated the dynamic analysis until the calculated final dislocation became nearly equal to the recorded value (Fig. 1). The finite element mesh used for the crust-fault system is shown in Fig. 5, and the model constants summarized in Table 1. The number of elements are 430 and the number of freedoms 936. Ten joint elements are arranged along the fault.

The average stress drop, $\Delta\tau$, one of the assigned parameters, was calculated as 20 bar from the following equation [7,8];

$$\Delta\tau = 0.74 \cdot \mu \cdot U/W \qquad \cdots\cdots(1)$$

in which, μ is the shear modulus, U is the average final dislocation and W the width of the fault. The distributions of the yield stress, τ_y, the other assigned parameter, and of the stress drop,

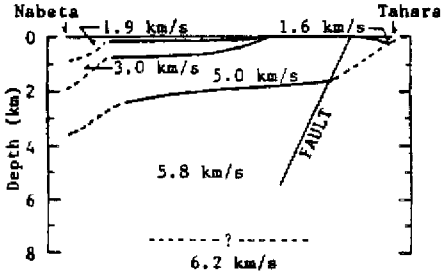

Fig. 4 Fault model and ground structure in the Mikawa area.

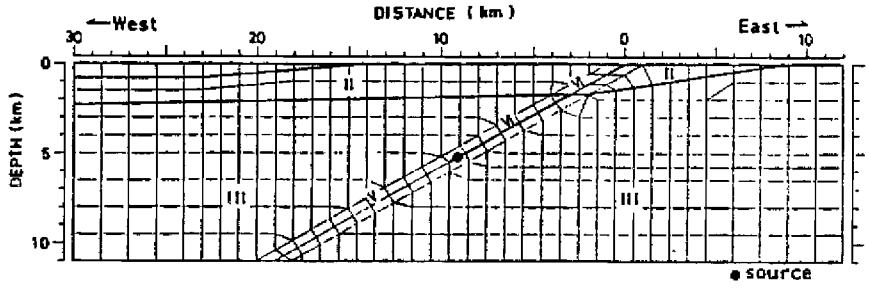

Fig. 5 Finite element mesh for calculation of the initial stress distribution and, analysis of the fault-rupture process.

Table 1 Parameters of the ground structure and the fault.

Crust	Unit weight (tf/m³)	Vp (km/s)	Vs (km/s)	Damping factor
I	2.0	2.0	1.0	0.0100
II	2.3	5.0	2.8	0.0033
III	2.5	5.8	3.4	0.0025

$\Delta\tau$, are assumed from the distribution of the initial stress as shown later (see Fig. 6).

4. RESULTS OF THE ANALYSIS AND THE ESTIMATION OF SEISMIC INTENSITY

4.1. *Results of static and dynamic analyses*

The distribution of the initial shear stress along the fault obtained from the static analysis is shown in Fig. 6. The distribution of the shear strength (yield stress) also is shown. The origin and position of the fault rupture in the lower layer where the initial stress exceeds the shear strength is designated by symbol ● in the figure.

The source-time function that denotes the time trace of the development of dislocation at ground surface is shown in Fig. 7. After the rupture front reached ground surface, the dislocation increased sharply to about 1.8 m within 3 seconds. Thereafter, dislocation was gradual and was complete by 40 sec. The final dislocation at ground surface was 2.08 m. This value approximates the recorded value of 2.2 m. The discussions in the following sections are based on the results of this analysis.

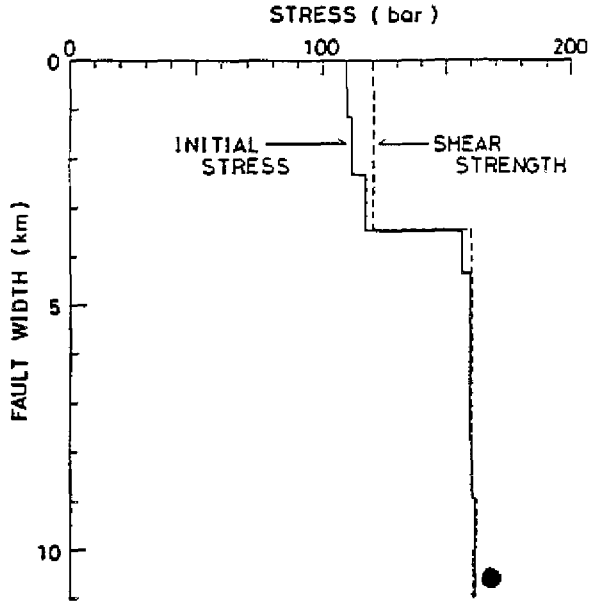

Fig. 6 Initial shear stress and shear strength distribution along the fault plane.

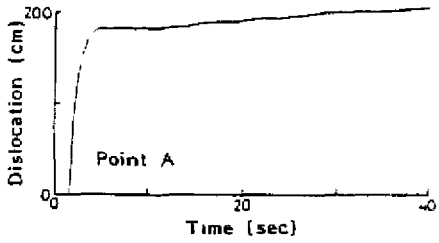

Fig. 7 Calculated source-time function at ground surface.

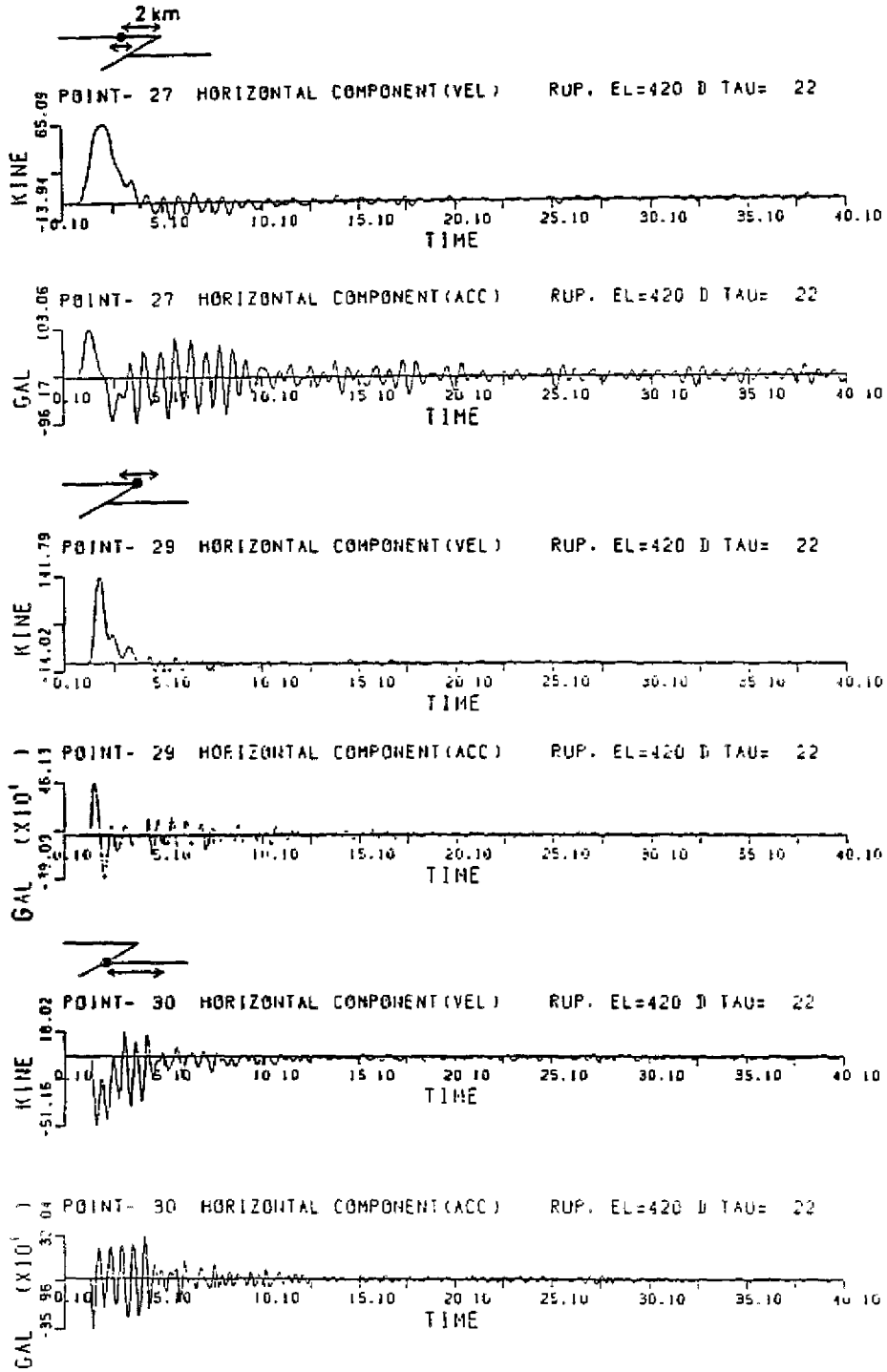

Fig. 8 Deformation curves for the horizontal component.

4.2. *Estimation of seismic intensity*

Time history curves obtained from the analysis made at and near the outcropping of the fault are shown in Fig. 8. The main shocks of acceleration continue for 10 seconds and those of the velocity only for 3 seconds. Moreover, the shape of the velocity curve during the main shock is almost single in terms of pulse. This is very important when considering the relation between ground motion and the disasters it causes.

In general, the JMA (Japan Meteorological Agency) intensity is related to maximum ground acceleration; but, this relation is valid only for ground motion with a predominant period of less than 1 second. When the predominant period is longer than that, there is a better correspondence between the intensity and the maximum velocity [9]. This relation is shown in Table 2. Fig. 8 shows that the predominant periods of these accelrograms are longer than 1 second, therefore, the authors could use the relation between the intensity and maximum velocity.

The attenuation curve of the maximum velocity at ground surface is given in Fig. 9 The region for each of the intensities determined from Table 2 is also given in this figure. For the upper block (the left side of the fault in the figure) the JMA intensity is VII within 1 km of the outcropping of the fault, VI from 1 to 10 km, and V beyond 10 km. In contrast, for the lower block, the JMA intensity is VI within 3 km and V beyond 3 km. The intensity on the upper block is higher than on the lower one, which agrees with the general tendency for damage done by an earthquake to be more severe on the upper than on the lower block.

The authors next compared the above results and the recorded intensity shown in Fig. 10. This figure was mapped by Iida [2] from a field survey of the Mikawa seismic disaster that included destroyed houses and is based on the JMA intensity. According to this figure, for the upper

Table 2 Relation between the seismic intensity and the maximum acceleration and maximum velocity.

Seismic intensity (JMA)	Maximum acceleration (Gal)	Maximum velocity (kine)
I	0.8–2.5	0.1 –0.32
II	2.5–8.0	0.32–1.0
III	8.0–25	1.0 –3.2
IV	25–80	3.2 –10
V	80–250	10–32
VI	250–400	32–100
VII	400–	100–

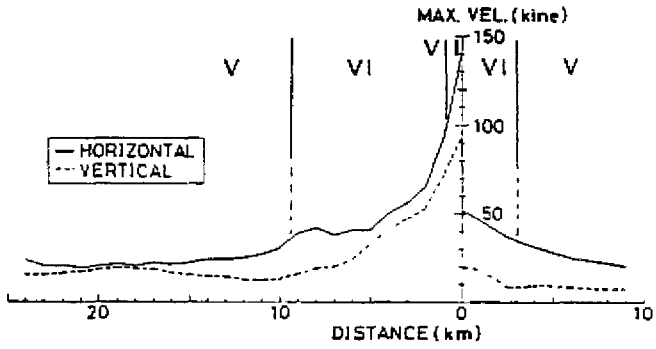

Fig. 9 Attenuation of peak velocity.

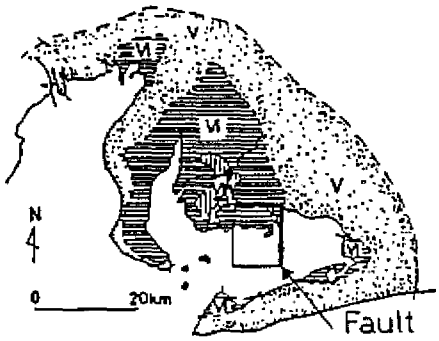

Fig. 10 Distribution of the recorded seismic intensity.

block, the intensity is VII on the fault and in other regions VI, except near the Yahagifuru River where the intensity is VII. For the lower block, the intensity is VI within of the outcropping of the fault. The analysis and the records for the region agree well within 10 km of the fault outcropping on the upper block and within 3 km on the lower block. For regions beyond those distances, the calculated seismic intensity is smaller than the recorded value. This discrepancy is attributable to lack of the amplification effect because of the soft surface ground use in the calculations. Accordingly, the authors took this effect into account in our calculations of seismic intensity First, we calculated the amplification factor of the surface ground by the multiple reflection theory, then multiplied this factor by the maximum velocity shown in Fig. 9. The resulting intensities are plotted in Figure 11, in which each city and town has been divided into 3 to 9 small zones and an intensity assigned to each zone. The general features of the distribution of the intensity in this figure closely resembles that in Fig 10. This shows the validity of our fault model and the method used to analyze ground motion.

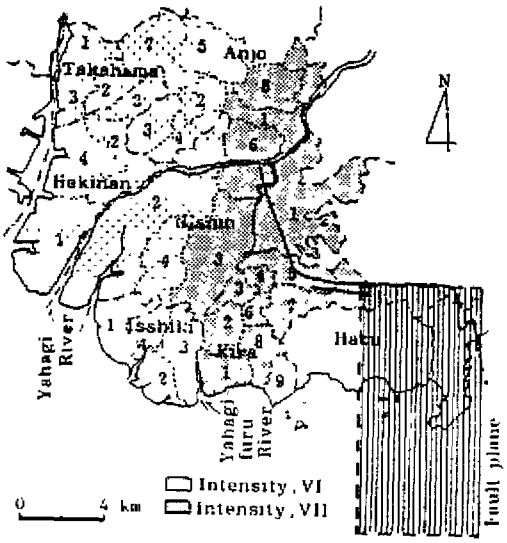

Fig 11 Distribution of seismic intensity evaluated on the basis of the calculated maximum velocity (see Fig. 9)

5. INVESTIGATION OF THE MIKAWA DISASTER BY QUESTIONNAIRE

5.1. *Outline of the questionnaire*

In order to determine the extent of liquefaction, the damage done to houses and the number and types of casualties, the authors distributed 2840 questionnaires to inhabitants of the West Mikawa area (shown by hatching in Fig. 12). Six cities and towns are included in the area. The survey was made on those who actually lived in the area and were more than twenty years old at the time of the 1945 Mikawa earthquake. Sixteen hundred and sixteen answers were collected (56.9% recovery).

5.2. *Liquefied sites*

According to the 1977 report [2], there were only a few liquefied sites. This is unnatural because the seismic intensity was very high near the fault and a soft alluvium deposit extended widely over the area; therefore, the potential for liquefaction is thought to have been very high In fact, we found from our questionnaire that there were many liquefied sites. Figs. 13, 14 and 15 show liquefied sites in Kira Town (Kira-cho), Isshiki Town (Isshiki-cho) and Nishio City.

The solid circles in all these figures and the hatched zones in Figs 14 and 15 denote liquefied points and zones. Solid squares show site where wells overflowed. These points and zones were determined from positions directly marked by answerers on maps which were distributed with the questionnaires. The large circles show liquefied points marked by more than three answerers, the small circles liquefied points marked by one or two answerers. In these figures, equi-depth contour line for the base of the alluvium deposit and the terrace (shadowed zone) also are given. Many liquefied points show up in the alluvium deposit plane in this city and the towns. In particular, liquefaction occurred over the entire alluvium deposit plane in Nishio City. In Isshiki Town, many liquefied points are located along the Yahagifuru River and in the west coastal zone.

5.3. *Damaged houses*

As examples, the damage done to wooden houses in Kira Town and in Nishio City is shown in Figs. 16 and 17. The damage ratio in percentage is given for each small zone shown in Fig. 11. Numbers allocated to the small zones are written at the left of the chart; from 1 to 9, Kira Town and from 1 to 4, Nishio City. The decimals at the right of the chart show the ratio of the rapidly demolished houses to the total number of destroyed (rapidly plus slowly demolished houses). This ratio hereafter called Wd.

In Kira Town, the rate of completely collapsed houses (rapidly plus slowly demolished houses)

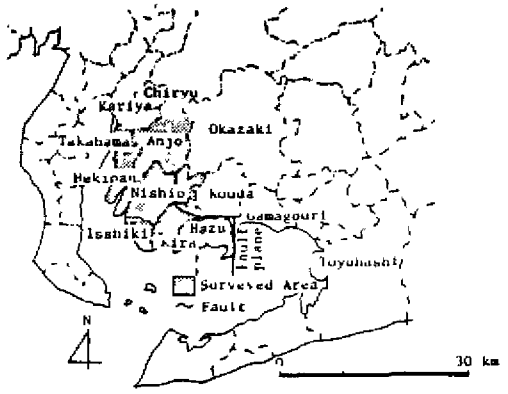

Fig. 12 Surveyed areas and the earthquake fault model.

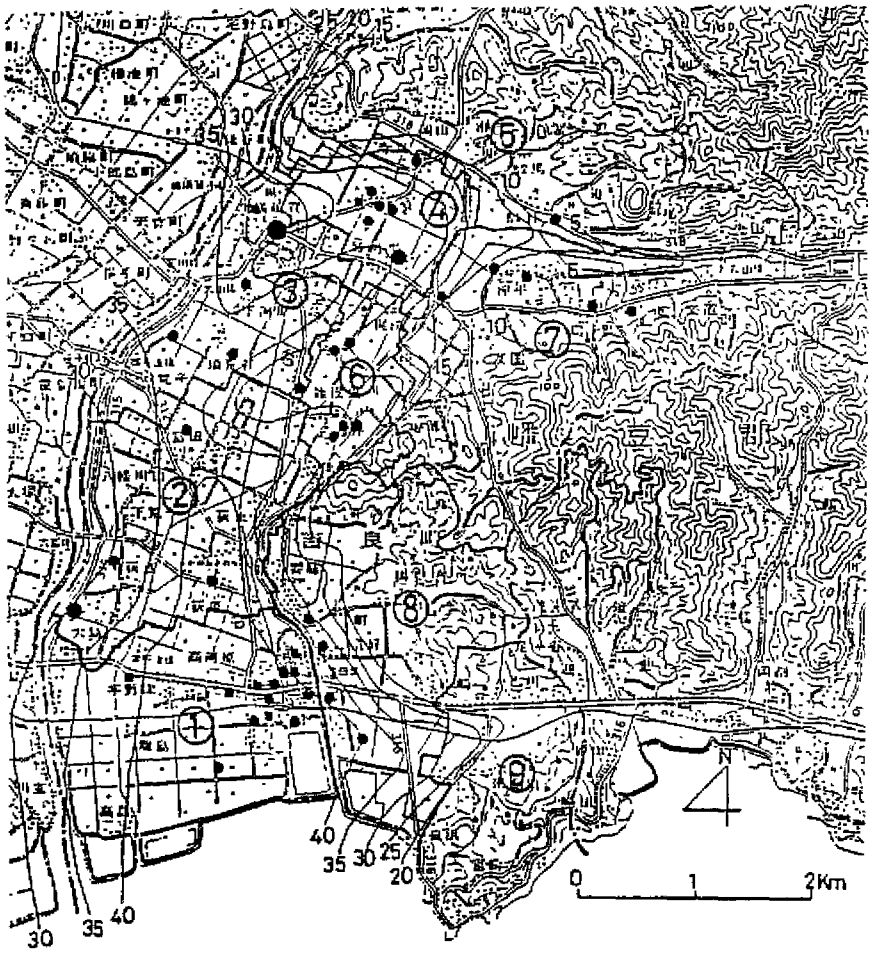

Fig. 13 Distribution of liquefied sites in Kira Town.

is highest in zone 4, about 65%. The value decreases in the order of zones 3, 2 and 1. The high percents in these zones are attributed to both strong ground motion and liquefaction. Zone 4 and 7 are located next to the fault. The Wd values in these zones are very high, 0.69 in zone 4 and 0.75 in zone 7. Although the ratio is higher in zone 7 than 4, the percent of completely collapsed houses is lower than in zone 4 because there was no liquefaction (see Fig. 13).

In Nishio City, the average rate of completely collapsed houses is a high 53.3%. In zone 3, the percent is highest, 69.3%, followed by zone 1, with 52.8%. These zones are close to the fault and liquefaction took place at many sites in them (see Fig. 15), which are the reason's for the high values. In contrast, zone 2 is closer to the fault than zone 4, but, the percent of destroyed houses is lowest in the city because there was little liquefaction in this zone The Wd values are very high in zones 3 and 1, 0.86 and 0.73; whereas, in zone 4 and 2 they are relatively low, 0 68 and 0.64. These values are considered high in comparison to those for Kira Town. On the basis of Figs 16 and 17 and the above discussion, the number of completely collapsed houses is shown to be strongly affected by liquefaction and for the ratio of rapidly demolished houses (Wd) to increases suddenly when the completely collapsed houses exceed 10%, the Wd becoming

Fig. 14 Distribution of liquefied sites in Isshiki Town.

more than 70–80% when at value exceeds 50%.

The relation between the maximum velocity and the percent of completely collapsed houses is shown in Fig. 18. A house is completely collapsed above 40 kines. In general, the ratio increases with the maximum velocity, there being two groups, A and B, in the relation. Zones belonging to group A are those in which liquefaction occurred are near the fault, or both. Zones belonging to B are in Hekinan City, Takahama City and mountainous area of Kira Town where liquefaction was rare.

5.4. *Casualties*

The number of answerers was 5464; men 46.3% and woman 51.7%. Table 3 lists the percent

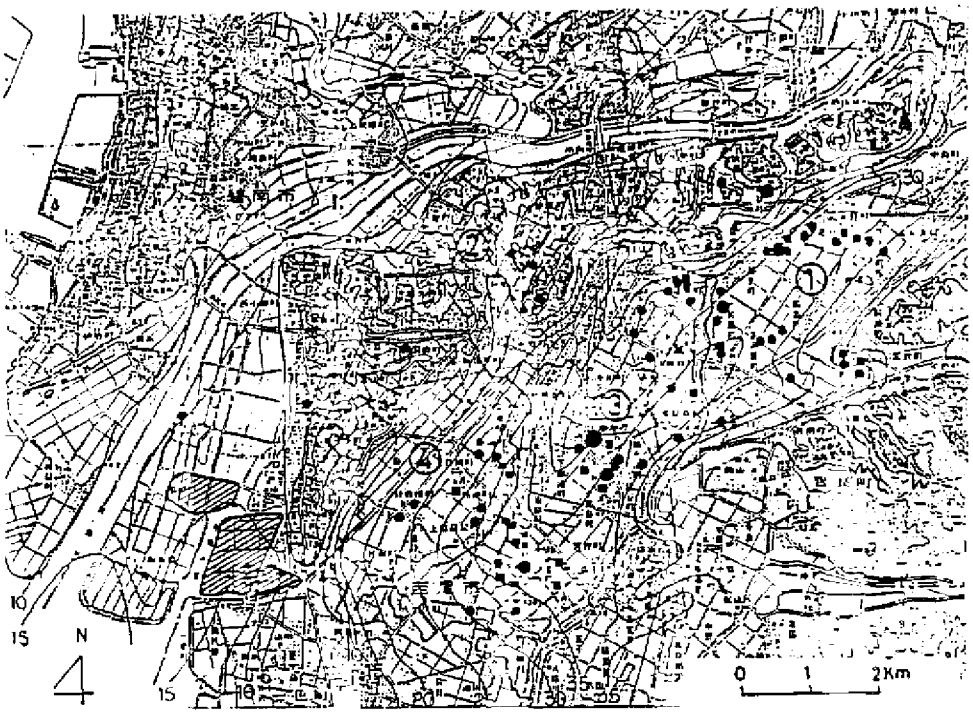

Fig. 15 Distribution of liquefied sites in Nishio City

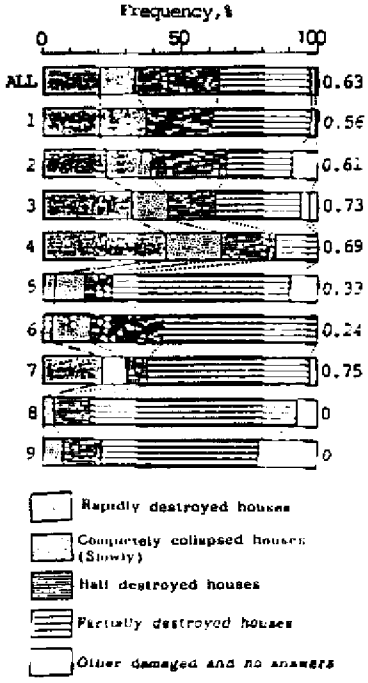

Fig. 16 Damaged wooden houses in Kira Town.

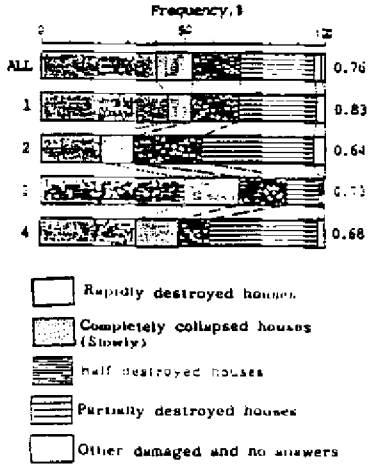

Fig. 17 Damaged wooden houses in Nishio City.

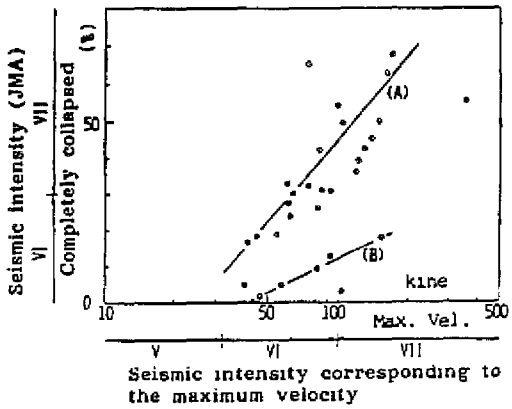

Fig. 18 Relation between maximum velocity and completely collapsed houses.

Table 3 Persons injured in each area by the 1945 Mikawa earthquake.

Surveyed area	Loss of life in percent	Percent of Injured	
		serious	slight
Kira	4.0	1.4	4.7
Nishio	6.0	2.9	8.4
Anjo	5.4	2.5	7.9
Isshiki	2.1	1.3	5.8
Takahama	0.2	0.7	3.3
Hekinan	0.2	0.1	1.8

of dead, seriously and slightly injured persons in each area affected by the Mikawa earthquake. The values for Nishio City are the highest; 6.0%, 2.9% and 8.4%. The values for Anjo City are the next highest.

The figures for the dead and injured in each area are compared with those for other earthquakes (Fig. 19). The value for the Mikawa earthquake is extremely high in comparison to

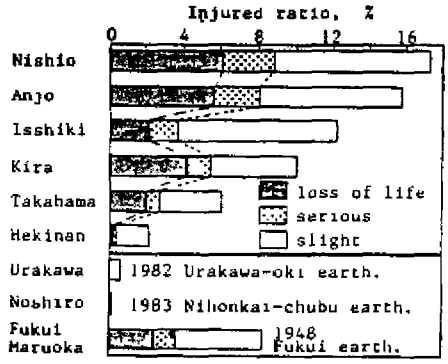

Fig. 19 Injured ratio from the Mikawa earthquake, and its comparison with other earthquake.

values found for recent earthquakes. For example, the value for casualties from the 1982 Urakawa-Oki earthquake is 0.7% in Urakawa Town where the JMA intensity was VI. It is 0.08% in Noshiro City where the JMA intensity was V for the 1983 Nihonkai-Chubu earthquake. Taking into account that the maximum JMA intensity is VII for the Mikawa earthquake, there is a tendency for the casualties value to increase by an order of one as the intensity increases on rank.

The JMA intensity in Fukui City and Maruoka Town in the 1948 Fukui earthquake was VII. Figure 11 shows intensity VII zones in Nishio City, Anjo City and Kira Town, in which the loss of life was more than 4%. In contrast, the figure was 2.4% for the Fukui earthquake. These values for the Mikawa earthquake are two to three fold the value for the Fukui earthquake. As casualties in the Mikawa earthquake mainly were caused by the destruction of houses, the difference in values can be attributed to the time the earthquake took place; the Mikawa earthquake took place at midnight, whereas the Fukui earthquake took place in the afternoon.

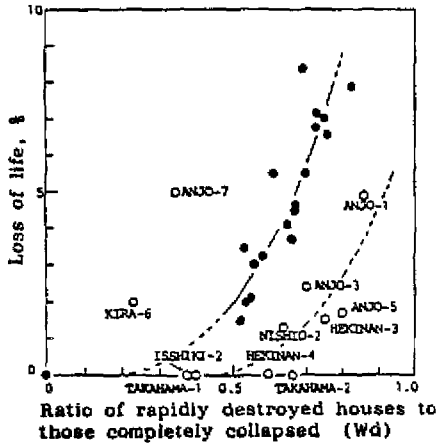

Fig. 20 Relation between the Wd (rapidly demolished house to the number of completely collapsed houses) and the loss of life.

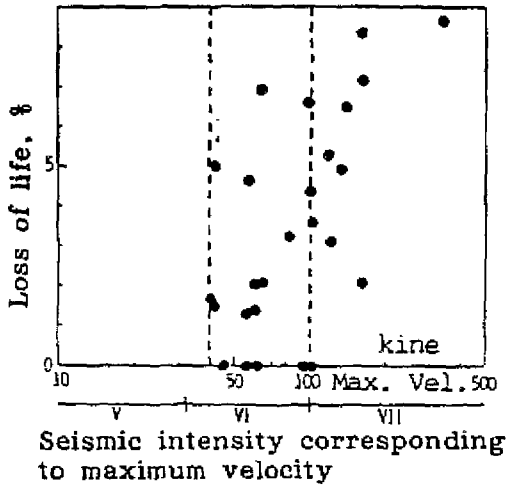

Fig. 21 Relation between the maximum velocity and loss of life.

The relation between the loss of life and rapidly demolished houses to the total number of destroyed houses is shown in Fig. 20. There are two groups as in Fig. 18. Zones belonging to the group of solid circles in Kira Town, Nishio City and Anjo City are located near the fault. In general, people were killed at more than 0.5 of Wd in the near and/or liquefied zones and loss of life increased sharply as the Wd increased.

On the other hand, people were killed at more than 0.6 of Wd in the regions belonging to the group of open circles, excepting zones Kira-6 and Anjo-7. In areas designated by open circles, there might be only a short time from the first excitation to the main shock because the sites are farther than the sites designated by solid circles. This made it possible for the inhabitants to take action quickly after the main shock and resulted in a lower loss of life in the open circle area for the same Wd value.

The authors have summarized the relation between the maximum velocity and the loss of life in Fig. 21. There is a tendency for the value denoting loss of life to increase as the maximum velocity increases. People would be killed at intensity VI, the loss of life being 0–7% for a seismic intensity of VI, and about 2–9% at intensity VII.

6. CONCLUSIONS

The authors have estimated the ground motion during the 1945 Mikawa earthquake and investigated the disaster caused by it. The ground motion was simulated by the nonlinear finite element method, and the disaster investigated by questionnaire. The relation between the intensity of the ground motion and the disaster was discussed. The main results were as follows.

(1) The distribution of seismic intensity in the Mikawa region estimated from the calculated maximum velocity gave a maximum intensity of VII near the earthquake fault and in the soft ground area in the south of the Mikawa region.

(2) The authors found many liquefied sites in Nishio City, Kira Town and Isshiki Town. The percent of damage to wooden houses and casualties in liquefied areas were greater than in nonliquefied areas.

(3) The relation between the loss of life and the JMA intensity, which is related to the maximum velocity, showed that people would be killed above intensity VI. Loss of life was 0–7% for intensity VI, but ranged from 2–9% for intensity VII. The value was higher than that for the Fukui earthquake which also had a maximum intensity of VII.

ACKNOWLEDGMENTS

The authors thank Prof. K. Toki, Disaster Prevention Research Institute, Kyoto University for his useful suggestions. We also are grateful to Mr. T. Tsuboi of Eiraku Fudousan Co., Ltd. for his help with the numerical calculations.

REFERENCES

[1] Rika Nenpyo (1985). Tokyo Astronomical Observatory, Maruzen Co., LTD, 799 pp. (in Japanese).

[2] Iida, K (1977). Seismic intensity distribution and damage to wooden houses in the Mikawa earthquake, Aichi Prefecture Committee for Disaster Prevention, pp. 1–96 (in Japanese).

[3] Toki, K and Miura, F. (1985). Simulation of a fault rupture mechanism by a two-dimensional finite element method, J of Phys. Earth, 33, pp. 485–511.

[4] Ando, M. (1974). Faulting in the Mikawa earthquake of 1945, Tectonophysics, Vol. 22 pp 173–186.

[5] Masaki, K. and Iida, K. (1981). On the ground structure of Nagoya area, I —Observation of seismic waves generated from the 1st Nagoya-Nabeta explosion—, Bull. of Aichi Inst. of Tech., Vol. 16B, pp. 165–173, (in Japanese).

[6] Masaki, K., Taniguchi, H. and Iida, K. (1982). On the ground structure of Nagoya Area, II —Observation of seismic waves generated from the 2nd Nagoya-Nabeta and the 1st Toyohashi-Tahara explosions—, Bull. of Aichi Inst. of Tech., Vol. 17B, pp. 159–171, (in Japanese).
[7] Knoppff, L. (1958). Energy release in earthquakes, Geophys. J. MNRAS. 1, pp. 44–52.
[8] Starr, A.T. (1928). Slip in a crystal and rupture in a solid due to shear, Proc. Camb. Phil. Soc., 24, pp. 485–500.
[9] Muramatsu, I. (1988). Investigation of the Relationship between Seismic Intensity and Earthquake Ground Motion, Proc., The Seismological Society of Japan, No. 1, pp. 280–281, (in Japanese).